

Generic model of an InAsSb/InAsSbP DH-LED for mid-infrared (2-5 μ m) applications

SANJEEV, P. CHAKRABARTI*

Department of Electronics and Instrumentation Engineering, Institute of Engineering and Technology, MJP Rohilkhand University, Bareilly -243 006 India

**Centre for Research in Microelectronics (CRME), Department of Electronics Engineering, Institute of Technology, Banaras Hindu University, Varanasi -221 005 India*

In this paper, we present a generic model of P⁺-InAs_{0.48}Sb_{0.22}P_{0.30}/ n⁰-InAs_{0.89}Sb_{0.11}/ N⁻-InAs_{0.48}Sb_{0.22}P_{0.30} double heterostructure light emitting diode (DH-LED) suitable for use as a source in absorption gas spectroscopy and futuristic optical fiber communication systems in the mid-infrared spectral region at 300K. The model takes into account all dominant radiative and non-radiative recombination processes, interfacial recombination and self-absorption in the active layer of the DH-LED structure. The proposed DH-LED has been studied for mid-infrared applications by considering the modulation bandwidth and its variation with active layer width, doping concentration, and injected carrier density. The rise time of the structure has been evaluated by considering the transient response for a step current of 50mA. The performance of the DH-LED has also been investigated at high carrier injection. The carrier leakage through the heterostructure, which affect the output power, is estimated in terms of confinement factor at high injection. The output power of the DH-LED has been computed as a function of bias current and compared/ contrasted with the reported experimental results.

(Received April 22, 2009; accepted June 15, 2009)

Keywords: Absorption gas spectroscopy, DH-LED, Mid-infrared, Optical fiber communication

1. Introduction

The mid-infrared region contains the fundamental finger print bands of a number of pollutants and toxic gases like NH₃ (2.1 μ m), HF (2.5 μ m), CH₄ (2.35 and 3.7 μ m), N₂O (3.9 and 4.5 μ m), hydrocarbon (3.3 μ m), SO₂ (4 μ m), CO₂ (4.2 μ m) and CO (4.6 μ m). These characteristics absorption properties of gases are used in the commercial gas detectors based on optical absorption spectroscopy [1-2]. Further, with the advent of polycrystalline metal halides such as Zinc Chloride (ZnCl₂), Thallium Bromide and Thallium Bromide (KRS-5) and heavy metal fluoride glass (HMFGL) such as ZBLAN, based optical fiber, which may offer a signal loss of less than 0.01dB/km in the mid infrared region [3]-[4], renewed research interest is created to explore suitable mid-infrared sources which can be used in the futuristic optical fiber communication systems. The mid-infrared sources require narrow bandgap semiconductor material for their fabrication. Fundamentally, the mid-infrared sources based on narrow bandgap semiconductors are subjected to strong non-radiative recombination, such as Shockley-Read-Hall (SRH) and Auger recombination, which adversely affect their quantum efficiency and prevent continuous room-temperature operation. The ternary III-V semiconductor alloy InAs_{1-x}Sb_x is a very promising material for the fabrication of mid-infrared light emitting diode as its energy gap covers the 3.5-5 μ m spectral range by suitably adjusting the mole-fraction x for the desired wavelength of operation. Various workers have fabricated the optimized mid-infrared light emitting diodes

for various target wavelengths useful for absorption gas spectroscopy and futuristic optical fiber communication systems but there is a lack of systematic theoretical study to characterize these sources for their applications in mid-infrared spectral region. It is, therefore, necessary to develop a generic model for the analysis of DH-LED operating in mid-infrared region. As the technology of narrow bandgap semiconductors is not yet fully mature and the cost of experimental investigation is high, there is a need for further theoretical studies in the area to advance the existing knowledge. The results of theoretical studies will provide useful design guidelines for improving and optimizing the existing structures and development of new device prototype.

2. Device structure

A schematic of the DH-LED structure is shown in Fig. 1 (a). It consists of two cladding layers of large bandgap quaternary material InAs_{0.48}Sb_{0.22}P_{0.30} of different conductivities and an active layer of InAs_{0.89}Sb_{0.11} sandwiched between them to form the double heterostructure. The InAs_{0.94}Sb_{0.06} buffer layer helps to reduce the large lattice mismatch (0.76%) between substrate (InAs) and cladding layer to nearly 0.41%. The proposed structure is expected to show the electroluminescence at 4.2 μ m at room temperature matching with the characteristic absorption wavelength of CO gas. The energy band diagram of the heterojunction has been obtained by applying the Anderson's model [5].

According to this model, the proposed structure forms the staggered Type-IIb band alignment. The energy band diagram of the structure is shown in Fig. 1(b).

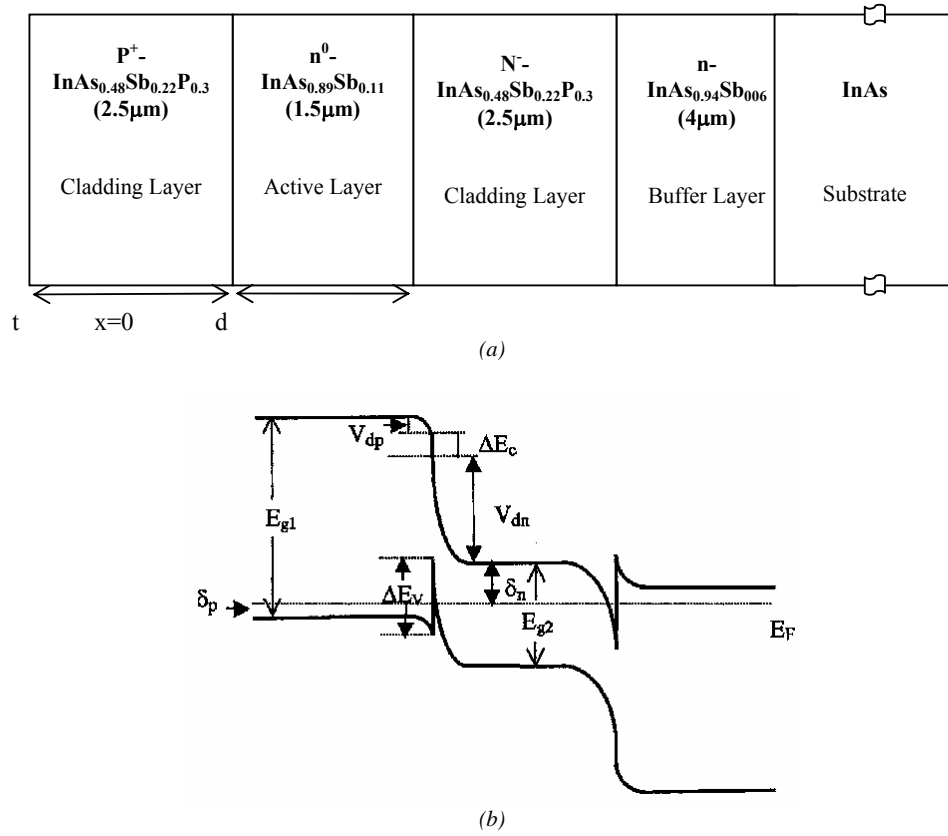


Fig. 1. (a) Schematic of the proposed DH-LED (b) Energy band diagram.

The energy bandgaps of the two semiconductors, their valance and conduction bandedge discontinuity and built-in-potential at n^0 - P^+ heterointerface after formation of heterojunction are related as

$$V_d = V_{dn} + V_{dp} \quad (1)$$

$$\Delta E_c = \chi_2 - \chi_1 \quad (2)$$

$$\Delta E_g = E_{g1} - E_{g2} \quad (3)$$

$$\Delta E_g = \Delta E_c + \Delta E_v \quad (4)$$

$$\delta_p + \delta_n + V_d + \Delta E_c = E_{g1} \quad (5)$$

where, V_{dn}, V_{dp}, V_d are the built-in potentials on n^0 and P^+ sides and the total built-in-potential respectively, ΔE_g is the total band-edge discontinuity, χ_1 and χ_2 are the electron affinity values of the wide and narrow bandgap semiconductor respectively, E_{g1} and E_{g2} are their

respective energy bandgaps, δ_n and δ_p are the separation between the Fermi level and band edge on n^0 and P^+ side respectively.

3. Formation of the model

The charge continuity equation of DH-LED in active region under forward bias is governed by [6]

$$\nabla^2(\Delta p(x)) = \frac{\Delta p(x)}{L_p^2} \quad (6)$$

where $\Delta p(x)$ is the injected hole density, L_p is the hole diffusion length given by $L_p = \sqrt{D_p \tau}$, D_p is the hole diffusion constant and τ is the lifetime of holes. Equation (6) can be solved analytically using the appropriate boundary conditions given by

$$\left. \frac{d(\Delta p(x))}{dx} \right|_{x=0} = \frac{J}{qD_p} - \frac{s_1}{D_p} \Delta p(0) \quad (7)$$

$$\left. \frac{d(\Delta p(x))}{dx} \right|_{x=d} = \frac{s_2}{D_p} \Delta p(d) \quad (8)$$

where J is the injected current density, q is the electronic charge, d is the thickness of active layer and s_1, s_2 are the surface recombination velocities at the P⁺-n⁰ and N⁺-n⁰ heterojunctions respectively. The hole density in the active region is calculated using (6), (7) and (8) as

$$\Delta p(x) = \frac{JL_p}{qD_p} \left[\frac{\cosh\left(\frac{d-x}{L_p}\right) + \frac{L_p s_2}{D_p} \sinh\left(\frac{d-x}{L_p}\right)}{\left[\left(\frac{L_p}{D_p}\right)^2 s_1 s_2 + 1\right] \sinh\left(\frac{d}{L_p}\right) + \frac{L_p(s_1 + s_2)}{D_p} \cosh\left(\frac{d}{L_p}\right)} \right] \quad (9)$$

The average hole density in the active region is given by

$$\overline{\Delta p} = \frac{1}{d} \int_0^d \Delta p(x) dx = \frac{J}{q} \frac{\tau_e}{d} \quad (10)$$

where τ_e is the effective carrier lifetime when surface recombination is important and is given by

$$\tau_e = \tau \left[\frac{\sinh\left(\frac{d}{L_p}\right) + \frac{L_p s_2}{D_p} \left[\cosh\left(\frac{d}{L_p}\right) - 1 \right]}{\left[\left(\frac{L_p}{D_p}\right)^2 s_1 s_2 + 1\right] \sinh\left(\frac{d}{L_p}\right) + \frac{L_p(s_1 + s_2)}{D_p} \cosh\left(\frac{d}{L_p}\right)} \right] \quad (11)$$

where τ is the net minority carrier lifetime due to radiative and non-radiative bulk recombination.

3.1 Lifetime modeling

In order to calculate the dominant current components of DH-LED and to analyze the structure in terms of output power and modulation bandwidth, it is necessary to model various radiative and non-radiative recombination lifetimes of the carriers in the active region of the proposed DH-LED. We have taken into account all the three dominant recombination processes e.g., radiative, Auger and Shockley-Read-Hall (SRH) recombination mechanisms for computation of minority carrier lifetime.

The SRH recombination can be largely controlled by improving the processing of the device while the Auger recombination lifetime is found to be dominating at room temperature for narrow bandgap materials. The modeling of the radiative recombination is rather straightforward.

For direct band semiconductor, the radiative lifetime of the carrier can be expressed as

$$\tau_R = \frac{1}{B_r(n_0 + p_0)} \quad (12)$$

where B_r is the radiative recombination coefficient of the material of active region, n_0 and p_0 are the electron and hole concentration in the active region under thermal equilibrium.

The modeling of Auger recombination lifetime is complex in nature. In the present model, we have assumed that the Auger processes involved in this structure follow those observed in InSb-like band structure. For the sake of simplicity we have considered the three dominant Auger mechanisms e.g., Auger-1 (A-1) or CHCC process, Auger-7(A-7) or CHLH process and Auger-S (A-S) or CHSH process in the active region. The first two transitions occur at the lowest threshold energy ($E_{th} \cong E_g$) and the last transition is dominating in the material in which the spin split energy gap (Δ) is nearly equal to forbidden gap. In the structure under consideration, $\Delta = 0.41 eV$ which is close to the value of forbidden gap. Therefore, we have considered the effect of Auger-S recombination in the model. The lifetime of the carrier corresponding A-1, A-7 and A-S are given by [7]

$$\tau_{A-1} = \frac{2\tau_{A-1}^i}{1 + n_0/p_0} \quad (13)$$

$$\tau_{A-7} = \frac{2\tau_{A-7}^i}{1 + p_0/n_0} \quad (14)$$

$$\tau_{A-S} = \frac{2\tau_{A-S}^i}{1 + p_0/n_0} \quad (15)$$

where $\tau_{A-1}^i, \tau_{A-7}^i, \tau_{A-S}^i$ are the values of lifetime involving the above three Auger processes for the intrinsic materials, given by

$$\tau_{A-1}^i = \frac{3.8 \times 10^{-18} \epsilon_s^2 (1 + \mu)^{1/2} (1 + 2\mu) \exp\left[\left(\frac{1 + 2\mu}{1 + \mu}\right) \frac{qE_{g2}}{kT}\right]}{\frac{m_e^*}{m_0} |F_1 F_2|^2 \left(\frac{kT}{qE_{g2}}\right)^{3/2}} \quad (16)$$

$$\tau_{A-7}^i = \frac{m_e^*(E_{th}) \left(1 - \frac{5qE_{th}}{4kT}\right)}{m_{e0}^* \left(1 - \frac{3qE_{th}}{2kT}\right)} \tau_{A-1}^i \quad (17)$$

$$\tau_{A-S}^i = \frac{5}{54} \frac{\epsilon_s^2 m_{hh}^* m_e^{*3/2} kT \mathcal{A} (E_{g2} + \Delta)}{\pi^4 \hbar^3 q^4 n_i^2 m_s^{5/2} (\Delta - E_{g2}) \exp\left[\frac{q(\Delta - E_{g2})}{kT}\right]} \quad (18)$$

Here, μ is the ratio of the conduction band to the heavy-hole valance band effective mass, ϵ_s is the permittivity, F_1 and F_2 are the overlap integrals of the periodic part of Bloch's functions, m_e^* is the electronic effective mass, m_0 is the electron rest mass, and n_i is the intrinsic carrier concentration, E_{g2} and Δ are the energy bandgap and spin-split-off energy of the material of the active region, $m_e^*(E_{th})$ is the electron effective mass corresponding to threshold energy for the Auger-7 transition. For this transition $E_{th} \approx E_{g2}$. For Auger-S transition m_{hh}^* and m_s correspond to the heavy-hole band effective mass and the spin-off band effective mass respectively [8-9].

The overall Auger lifetime value involving the three Auger processes can be obtained as

$$\frac{1}{\tau_A} = \frac{1}{\tau_{A-1}} + \frac{1}{\tau_{A-7}} + \frac{1}{\tau_{A-S}} \quad (19)$$

The lifetimes of minority carriers due to Shockley-Read-Hall (SRH) recombination can be modeled in terms of SRH trap-density and capture cross-section as

$$\tau_{SRH} = \frac{1}{\sigma N_f v_{th}} \quad (20)$$

where N_f is the SRH trap density, σ is the capture cross-section. Here v_{th} is the thermal carrier velocity of the minority carriers in the active region given by

$$v_{th} = \sqrt{\frac{3kT}{m_e^*}} \quad (21)$$

where m_e^* is the electron effective mass. The net value of the carrier lifetime τ can be obtained as

$$\frac{1}{\tau} = \frac{1}{\tau_R} + \frac{1}{\tau_A} + \frac{1}{\tau_{SRH}} \quad (22)$$

3.2 The current-voltage characteristics of the structure

The current through the forward bias DH-LED consists of two components

(i) Diffusion current arising from the minority carriers injected from neutral P^+ and n^0 regions. (ii) Drift current due to generation recombination in the depletion region at $P^+ - n^0$ junction.

3.2.1 The diffusion component

Due to the presence of discontinuities in the bandages at the heterointerface, the diffusion currents in heterostructure are different from that in homojunction. In the given structure, electrons having energy equal to $V_d + \Delta E_c$ can reach the heterointerface of P^+ region and similarly the holes from P^+ region, having energy equal to the barrier $V_d - \Delta E_v$ can reach to the interface at n^0 region to constitute the total diffusion component of the current in the structure. The diffusion components of current due to injection of electrons and holes in P^+ and n^0 regions injected from n^0 and P^+ region respectively can be obtained by solving equation (6) under appropriate boundary conditions as

$$I_{sn} = q \frac{AL_n}{\tau_e} n_{p0} \frac{\frac{L_n s_1}{D_n} \cosh\left(\frac{d-x_p}{L_n}\right) + \sinh\left(\frac{d-x_p}{L_n}\right)}{\frac{L_n s_1}{D_n} \sinh\left(\frac{d-x_p}{L_n}\right) + \cosh\left(\frac{d-x_p}{L_n}\right)} \exp\left[-\frac{q(V_d + \Delta E_c)}{kT}\right] \quad (23)$$

$$I_{sp} = q \frac{AL_p}{\tau_e} p_{n0} \frac{\frac{L_p s_2}{D_p} \cosh\left(\frac{t-x_n}{L_p}\right) + \sinh\left(\frac{t-x_n}{L_p}\right)}{\frac{L_p s_2}{D_p} \sinh\left(\frac{t-x_n}{L_p}\right) + \cosh\left(\frac{t-x_n}{L_p}\right)} \exp\left[-\frac{q(V_d - \Delta E_v)}{kT}\right] \quad (24)$$

where n_{p0} and p_{n0} are the minority carrier concentration in P^+ and n^0 regions at equilibrium, L_n and L_p are the diffusion lengths for electrons and holes respectively, D_n and D_p are their respective diffusion coefficients. A is the area of the junction and x_n and x_p are the widths of the depletion region on the respective sides [10].

The total diffusion current component under an applied voltage V for the structure is given by

$$I_d = (I_{sn} + I_{sp}) \exp\left[\frac{qV}{kT} - 1\right] \quad (25)$$

3.2.2 The generation-recombination component

The carriers generated in the depletion region are generally separated under the application of existing electric field. The transport of carriers across the heterojunction is strongly affected by the trap levels at the heterointerface inside the depletion region. The carrier generation-recombination in the active region is governed by the Shockley-Read-Hall equation. The electron and hole components of current arising from the generation-recombination in the depletion region under forward bias is given by [11]

$$I_{gr} = \frac{2n_i W A k T}{(V_d - V) \tau_{SRH}} \sinh\left(\frac{qV}{2kT}\right) \quad (26)$$

where V_d is the total built-in-potential, V is the applied voltage, W is the total depletion width which is the function of applied voltage V , n_i is the intrinsic carrier concentration of the active region and τ_{SRH} is the SRH generation-recombination lifetime.

3.3 Output power and modulation bandwidth

The output power of the DH-LED taking the interfacial recombination, self-absorption and effect of high carrier injection into consideration can be given by

$$P = \eta h \nu \left(\frac{I}{q}\right) \quad (27)$$

where η is the quantum efficiency of the LED, I is the bias current.

The 3-dB modulation bandwidth (f_{3dB}) of DH-LED can be calculated as

$$f_{3dB} = \frac{I}{2\pi\tau_e} \quad (28)$$

4. Performance of the proposed DH-LED at high carrier injection

In this section, the effect of injected carrier density on the performance of the DH-LED has been modeled.

4.1 Effect of high carrier injection on carrier lifetime

Both radiative and non-radiative minority carrier lifetimes are affected significantly in the case of high level injection of minority carriers in the active region.

In presence of excess carrier (Δp), the radiative lifetime can be expressed as

$$\tau'_R = \frac{I}{B_r(n_0 + p_0 + \Delta p)} \quad (29)$$

where Δp is given by

$$\Delta p = \left(\frac{J\tau'_R}{qd}\right) \quad (30)$$

Here J is the injected current density. Solving (29) and (30) for the value of radiative recombination lifetime, we obtain

$$\tau'_R = \frac{\left[(n_0 + p_0)^2 + \frac{4J}{B_r qd}\right]^{1/2} - (n_0 + p_0)}{2J/qd} \quad (31)$$

Under the high injection condition, the lifetime values of three Auger processes can be obtained as [7]

$$\tau'_{A-1} = \frac{2n_i^2 \tau_{A-1}^i}{(n_0 + p_0 + \Delta p)[(n_0 + \Delta p) + \gamma(p_0 + \Delta p)]} \quad (32)$$

$$\tau'_{A-7} = \frac{2n_i^2 \tau_{A-7}^i}{(n_0 + p_0 + \Delta p)(p_0 + \Delta p)} \quad (33)$$

$$\tau'_{A-s} = \frac{2\tau_{A-s}^i}{1 + ((p_0 + \Delta p)/(n_0 + \Delta p))^2} \quad (34)$$

where factor γ accounts for the hole-hole collisions and is given by

$$\gamma = \frac{\mu^{1/2}(1 + 2\mu)}{2 + \mu} \exp\left[-\left(\frac{1 - \mu}{1 + \mu}\right) \frac{qE_{g2}}{kT}\right] \quad (35)$$

4.2 Carrier leakage at high injection level

In the calculation of output power from DH-LED, it is assumed that hetero-junction barrier height is large enough to ensure that carriers are confined into the active region. But when the active layer thickness is low or junction temperature rises or injection level is high, there are chances that injected carrier may leak through the heterostructure barriers. The extent to which the carrier confinement can take place is given by confinement factor (C) defined as [12]

$$C = \frac{J}{(J' + J)} \quad (36)$$

where J is the current density due to injected carrier and J' is the excess current density due to diffusion and drift component of electrons and holes required to keep the constant injected carrier density in the active region.

5. Transient analysis of proposed structure

In order to achieve the high modulation bandwidth it is necessary that rise time of the DH-LED should be low. The rise time of the structure has been estimated by the transient behavior when a current step function of amplitude I_T is applied to it. The differential equation for the diffusion current [13-14] is

$$\frac{dI}{dt_n} = \frac{\beta\tau_e I_0(I+1)(I_T - I)}{C_s + \beta\tau_e I_0(I+1)} \quad (37)$$

in which I_0 is the saturation current, $\beta = q/2kT$, $t_n = t/\tau_e$, τ_e is the effective lifetime, $I = I_d/I_0$ and $I_T = I_T/I_0$, I_d is diffusion current, and I_T is the magnitude of step current. The integration of equation (37) gives the variation of I with τ as follows

$$t_n = \left(\frac{C_s}{\beta\tau_e I_T} \right) \log_e I - \left[I + \left(\frac{C_s}{\beta\tau_e I_T} \right) \right] \log_e \left(I - \frac{I_d}{I_T} \right) \quad (38)$$

The 10 to 90% rise time t_R is calculated as

$$t_R = \left[\tau_e + \left(\frac{2C_s}{\beta I_T} \right) \right] \log(9) \quad (39)$$

6. Results and discussion

Numerical computation has been carried out for $P^+ - \text{InAs}_{0.48}\text{Sb}_{0.22}\text{P}_{0.30} / n^0 - \text{InAs}_{0.89}\text{Sb}_{0.11} / N^- - \text{InAs}_{0.48}\text{Sb}_{0.22}\text{P}_{0.30}$ double heterostructure light emitting diode (DH-LED) at 300K. In the analysis we have considered equal surface recombination velocity at both the heterointerfaces i.e. $s_1 = s_2 = s$. The various parameters used in the model are summarized in Table 1. Some of the parameters of the quaternary materials (InAsSbP) have been computed from the parameters of the constituent binary/ternary materials using the linear interpolation technique.

Table 1. Values of parameters used in the model [15], [16].

Parameter	Value
N_A	10^{24}m^{-3}
N_D	10^{22}m^{-3}
N_f	10^{20}m^{-3}
σ	10^{-19}m^2
t	$2.5 \mu\text{m}$
d	$1.5 \mu\text{m}$
E_{g1}	0.49 eV (computed)
E_{g2}	0.2731 eV (computed)
χ_1	4.73 eV (computed)
χ_2	4.86 eV
m_n^* (InAs _{1-x} Sb _x)	$(0.023-0.039x+0.03x^2)m_0$
m_p^* (InAs _{1-x} Sb _x)	$(0.026-0.011x)m_0$
m_s (InAs _{1-x} Sb _x)	$(0.16-0.04x)m_0$
m_{hh} (InAs _{1-x} Sb _x)	$(0.41+0.02x)m_0$
Δ (InAs _{1-x} Sb _x)	$(0.39-0.75x+1.17x^2) \text{eV}$

Fig. 2 depicts the forward-bias current-voltage characteristics of the proposed structure. The graph shows the usual exponential rise in the current with the increase in the applied voltage. The cut-in-voltage is approximately 0.27V.

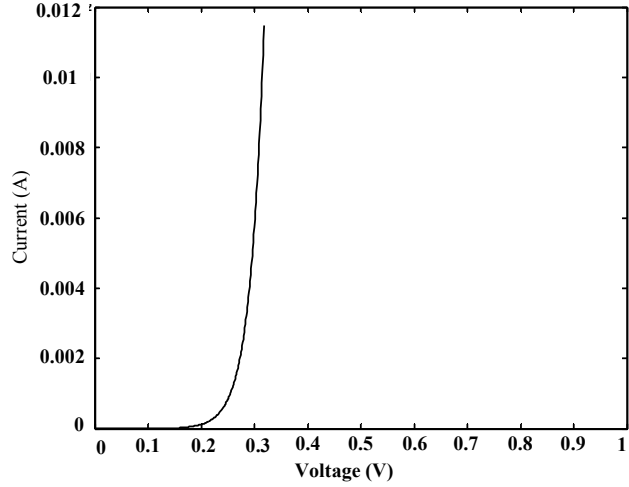


Fig. 2. Forward-bias current-voltage characteristics of the DH-LED.

Fig. 3 shows the variation of output power and bandwidth of DH-LED with normalized active layer width for two different values of surface recombination velocity. The output power decreases sharply from $30 \mu\text{W}$ to around $13 \mu\text{W}$ with an increase in the value of active layer thickness from $0.45 \mu\text{m}$ to $3.9 \mu\text{m}$ for $s=10 \text{m/s}$. For $s=100 \text{m/s}$ the output power decreases from $30 \mu\text{W}$ to around $6 \mu\text{W}$ for the same increment in the value of the normalized active layer thickness. Also for a given value of active layer thickness of $1.3 \mu\text{m}$ ($d=L_p$), the output power of DH-LED decreases from $16 \mu\text{W}$ to nearly $7 \mu\text{W}$ as we increase the surface recombination velocity from 10m/s to 100m/s while the bandwidth of the DH-LED increases from $1.5 \times 10^8 \text{Hz}$ to nearly $2.5 \times 10^8 \text{Hz}$. Also the bandwidth increases sharply from $1 \times 10^8 \text{Hz}$ to $3 \times 10^8 \text{Hz}$ as we increase the normalized active layer thickness from 0.5 to 2.5 for $s=10 \text{m/s}$. From the graph we have seen that, both surface recombination velocity and normalized active layer thickness have the opposite effect on the modulation bandwidth as on the output power of the DH-LED, so as to keep the power-bandwidth product constant. Further, the bandwidth of the structure increases with increase in the injected carrier density and doping concentration.

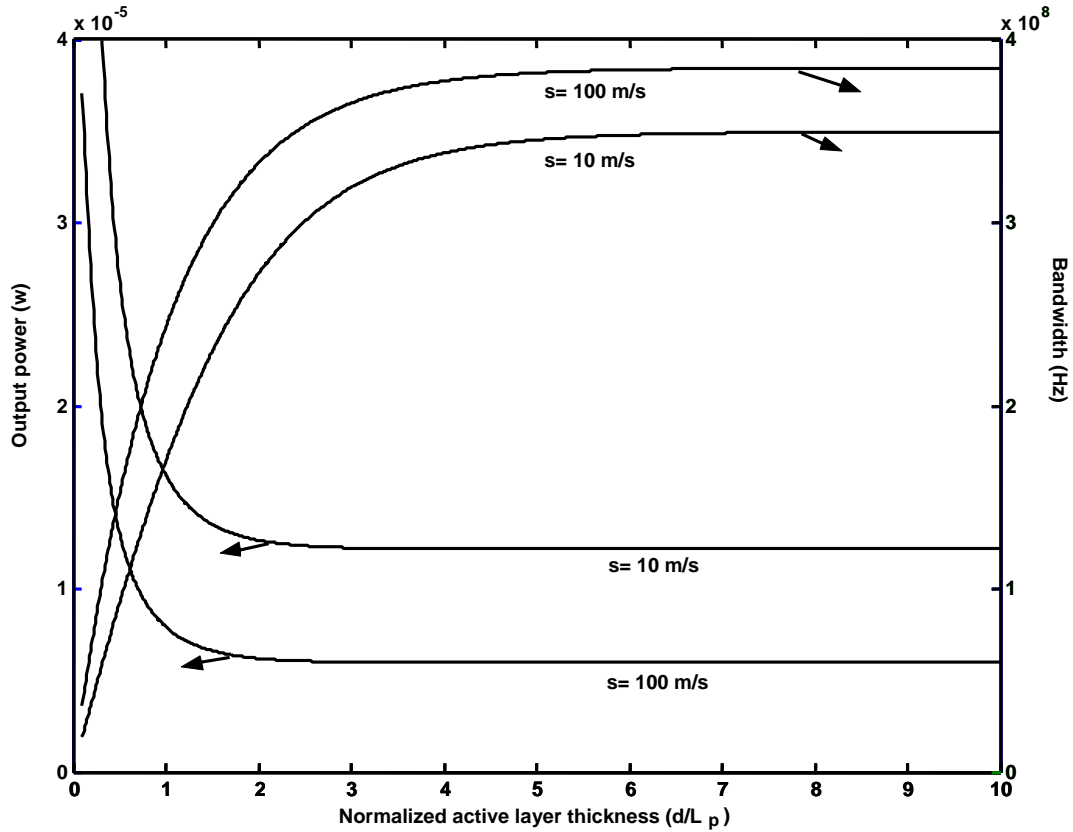


Fig. 3. Output power and bandwidth variation with normalized active layer thickness for different surface recombination velocities.

This is shown in Fig. 4. Fig 5 shows the variation of confinement factor for a given barrier height of the heterointerface with active layer thickness for different injected carrier density. It is clear from the graph that at higher injected carrier density, confinement is poor and carrier leakage through the heterostructure may take place. This in turn, reduces the output at high injection level.

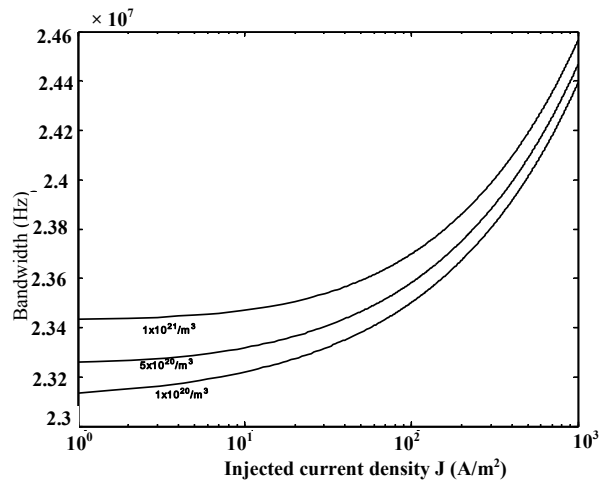


Fig. 4. Bandwidth variation with injected carrier density for different doping concentration.

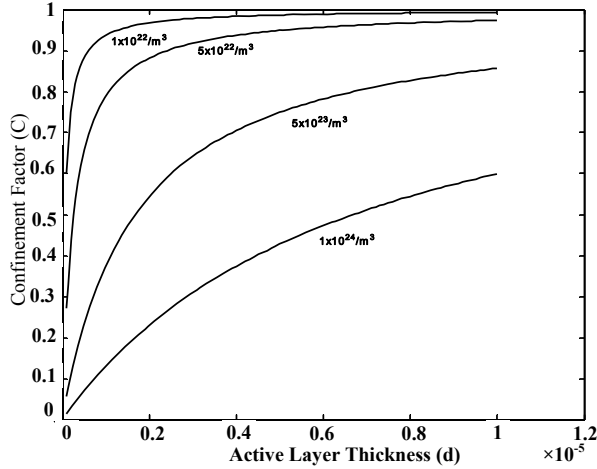


Fig. 5. Variation of confinement factor with active layer thickness for different injected carrier density.

Fig. 6 shows the variation of the Auger and radiative lifetime of the carriers with the excess injected carriers. It is seen that the lifetime of carriers decreases drastically with the increase in the excess injected carrier beyond $10^{24}/\text{m}^3$. It is also observed that Auger recombination lifetime is the dominating non-radiative recombination which affects the output power of DH-LED more severely.

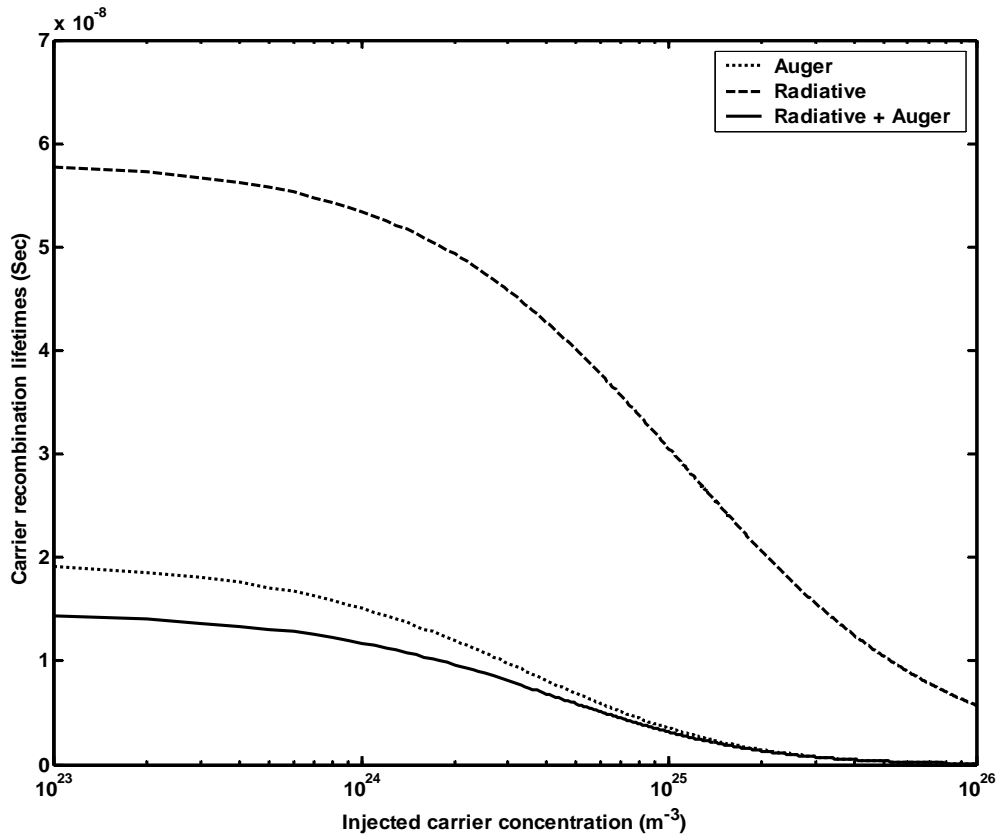


Fig. 6. Radiative and Auger recombination lifetime variation with injected carrier concentration.

Fig. 7 shows the variation of optical power output of DH-LED estimated with and without considering the high carrier injection effect, with the bias current. It is seen that there is a poor matching between the experimental and theoretical results calculated when we do not take the high

carrier injection effect on the output power of the DH-LED in consideration. The theoretical results which take into account the high carrier injection effect are in good agreement with the reported experimental results [15].

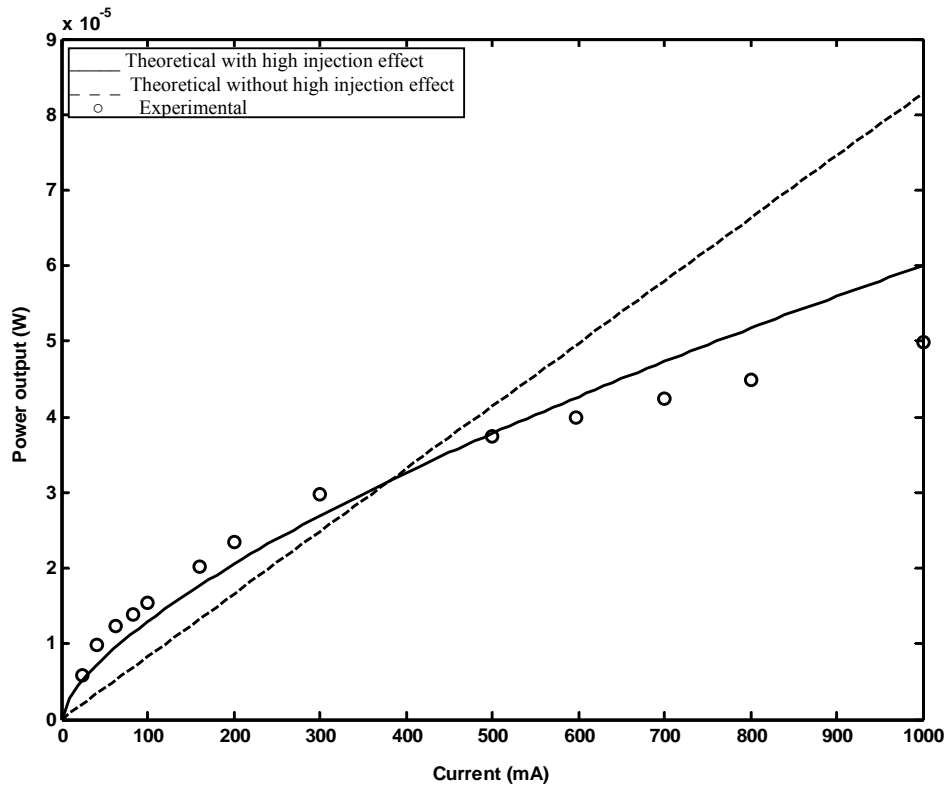


Fig. 7. Variation of optical power output of the DH-LED with the drive current.

The transient response of the LED for a 50mA step input current is shown in Fig. 8.

The rise time has been estimated to be 25.27 ns for the given structure.

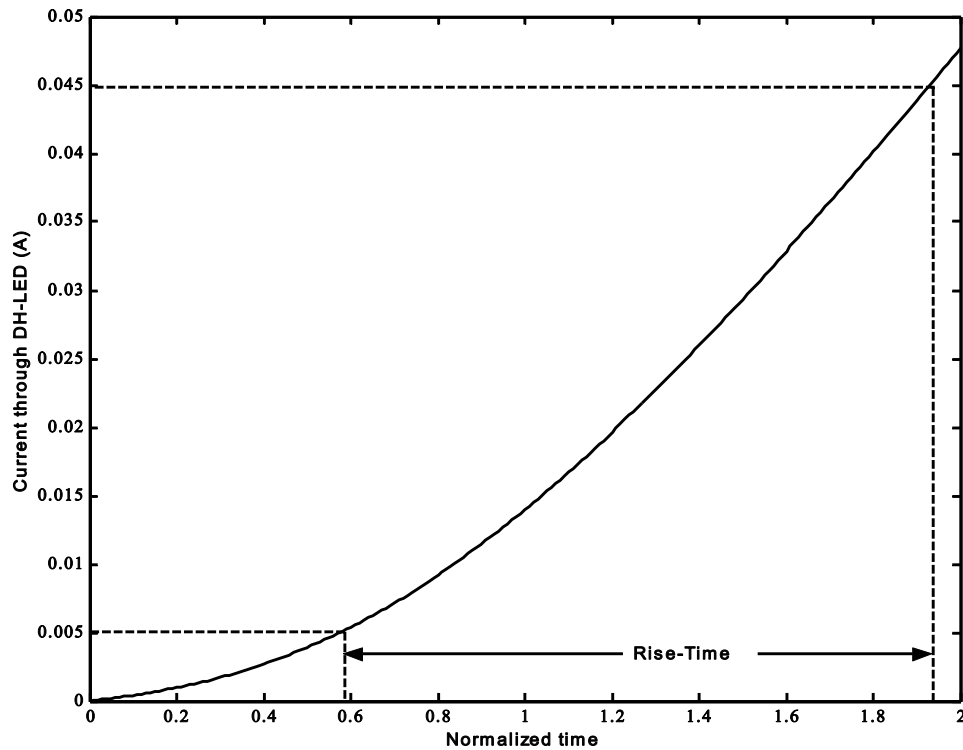


Fig. 8. Variation of current through DH-LED with time for an applied step current of 50mA.

The DH-LED has a reasonably small value of rise time which will make it suitable for high frequency modulation applications.

7. Conclusions

A generic physics-based model for a narrow bandgap III-V semiconductor DH-LED for mid-infrared has been developed for analyzing the device at room temperature. The results obtained on the basis of the model have been compared with the experimental reported results for the same structure and found to be in good agreement. The study reveals that high level of carrier injection results in a reduction in the effective lifetime which in turn causes the output power to saturate at higher bias current. The simulation codes developed here can be extended for the performance optimization of any other similar DH-LED in mid-infrared spectral region. The model developed here would also provide useful design guidelines to the experimentalists for developing new device prototypes.

Acknowledgements

One of the authors (Sanjeev) would like to acknowledge the financial support from the Council of Science and Technology, UP (CST-UP), Lucknow, India for this work in the form of a research project.

References

- [1] A. Krier, *Mid-infrared semiconductor optoelectronics*, Springer, 2006.
- [2] A. Krier, *Phil. Trans. R. Soc. Lond. A*, **359**, 599 (2001)
- [3] D. A. Pinnow, A. L. Gentile, A. G. Standlee, A. J. Timper, L. M. Hobrock, *Appl. Phys. Lett.* **33**, 28 (1978).
- [4] P. W. France, S. F. Carter, M. W. Moore, C. R. Day, *British Telecom Tech. J.* **5**, 28 (1987).
- [5] B. L. Sharma, R. K. Purohit, *Semiconductor Heterojunctions*, Pergamon, New York, 1974.
- [6] T. P. Lee, A. G. Dentai, *IEEE J. Quant. Electron. QE-* **14**, 150 (1978).
- [7] A. Rogalski, K. Adamiec, J. Rutkowski, *Narrow-Gap Semiconductor Photodiodes*, SPIE Press, Bellingham, 2000.
- [8] A. Rogalski, Z. Orman, *Infrared Phys.* **25**, 551 (1985).
- [9] Y. Tian, Z. Tianming, T. Zhou, B. Zhang, Y. Jin, Y. Ning, H. Jiang, G. Yuan, *Opt. Eng.* **37**, 1754 (1998).
- [10] Y. Tian, B. Zhang, T. Zhan, H. Jiang, Y. Jin, *IEEE Trans. Electron Devices. ED-* **47**, 544 (2000).
- [11] R. Scholar, S. Price, J. Rosbeck, *J. Vacuum Science and Tech. B* **10**, 1507 (1992).
- [12] J. Zucker, Robert B. Lauer, *IEEE Trans. Electron. Device ED-* **25**, 193 (1978).
- [13] C. J. Hwang, J. C. Dymont, *J. Appl. Phys.* **44**, 3240 (1973).
- [14] P. Chakrabarti, V. Saxena, S. K. Das, Y. S. Rao, B. Balaji Lal, *Opt. Quant. Electron.* **26**, 885 (1994).
- [15] H. H. Gao, A. Krier, V. Sherstnev, Y. Yakovlev, *J. Phys. D: Appl. Phys* **32**, 1768 (1999).
- [16] M. Levinshtein, S. Rumyantsev, M. Shur, *Handbook Series on Semiconductor Parameters* **2**, World Scientific, 1996.

Corresponding author: pchakra@bhu.ac.in